

Rotational Compliance Measurements of a Flexible Plane Structure Using an Attached Beam-like Tip, Part 2: Experimental Study

Y. C. Qu
Graduate Student.

L. Cheng
Associate Professor.

D. Rancourt
Assistant Professor.

Department of Mechanical Engineering,
Laval University, Québec, Canada, G1K 7P4

This paper presents an experimental assessment of the Tip Excitation Technique (TET) introduced in a companion paper. The aim of the technique is to measure the rotational compliance of attached plane structures. Following the guidelines established on the basis of a numerical study in the companion paper, experimental measurements were performed on a rectangular plate and results were compared with numerical simulations. The investigation focuses on the general performance of the technique, on the different types of excitation used and on other factors necessary to ensure accurate results. In addition, an error analysis is conducted to demonstrate the sensitivity of the results to biased measurement quantities. It is concluded that the proposed technique can be used in the low to middle frequency range, where relatively strong modal behavior is involved.

1 Introduction

In a companion paper, Cheng and Qu (1997) proposed a simple experimental technique, using an L-shaped beam-like tip, to estimate the rotational compliance of attached plane structures. It was shown that the technique overcomes difficulties encountered regarding the application of a moment excitation and measurement of the induced angular response. By measuring the translational acceleration at the top of the tip, fixed on the plane structure, the rotational compliance of the plane structure can be evaluated by using two simple expressions derived in the previous work. For the sake of convenience, we rewrite these two formulas as

$$A_{cr} = \frac{1}{\omega^2} \sqrt{\left(\frac{K}{T}\right)^2 - 2I_{yy} \frac{K}{T} \cos \phi_a + I_{yy}^2} \quad (1)$$

$$\tan \phi_{cr} = \frac{-I_{yy} \sin \phi_a}{I_{yy} - \frac{K}{T} \cos \phi_a} \quad (2)$$

where A_{cr} and ϕ_{cr} are, respectively, the amplitude and the phase angle of the rotational compliance; I_{yy} is the total effective moment of inertia of the tip; T and ϕ_a are respectively, the amplitude and the phase angle of the translational acceleration measured on the tip; and K is a geometric parameter which depends on the position of the excitation and that of the acceleration response.

Following the guidelines established in the previous work, a properly designed tip transforms a complicated rotational measurement problem into a classical translational one. As a result, once the translational acceleration is obtained in terms of the amplitude and phase angle, one can derive the amplitude and phase angle of the rotational compliance.

The TET was first of all validated using numerical simulations in the previous work. In the present paper, an experimental

investigation is carried out to further assess the technique and address the following issues: 1) the overall performance of the technique based on the experimental data; 2) the effects of different force excitation methods and other physical factors on the accuracy of the technique, and 3) an error analysis to show the sensitivity of the technique to variations in the measured quantities.

2 Experimental Set-up

A schematic diagram of the experimental set-up is shown in Fig. 1. The structure tested was a cantilever rectangular plate. Using the proposed technique, a beam-like tip was fixed at a given point along the free edge of the plate; the whole system is referred to as the "basic configuration" whose characteristics have already been given in the companion paper. The plate was horizontally attached to a rigidly fixed base. In order to provide a satisfactory clamped support, a wide-flange, mild steel (W150 × 24) I-shaped beam and a 10 mm thick steel strip, were used to clamp the plate with twelve M8 bolts. The base of the tip was screwed to the plate using three small M3 bolts in the position P whose coordinates, with respect to the $\bar{x}y\bar{z}$ system, are (400, -100, 0) in millimeters (cf. Fig. 1).

The block diagram of the experimental set-up is represented in Fig. 2. Two excitation methods were tested: impact excitation by a hammer and random excitation by an exciter. For the former, a B&K 8202 impact hammer equipped with the B&K 8200 force transducer was used (Broch 1984). For the latter, an HP 35660A Signal Analyzer was used to generate a broad band random signal which was then amplified by a power amplifier B&K (2706) to supply the exciter (B&K 4809). The excitation force was applied to the tested structure by a thin steel push-rod possessing very low lateral stiffness compared with its longitudinal stiffness, to avoid any moment excitation (cf. Fig. 4b). The driving force was measured using a force transducer B&K 8200. The tip acceleration induced by the excitation force was measured with a tiny accelerometer (B&K 4393), a charge amplifier (B&K 2626) and an HP 35660A Signal Analyzer. Data preprocessing and preparation were carried out with the analyzer. In the experiment, both the excitation and the

Contributed by the Technical Committee on Vibration and Sound for publication in the JOURNAL OF VIBRATION AND ACOUSTICS. Manuscript received Sept. 1994; revised Sept. 1995. Associate Technical Editor: J. Mottershead.

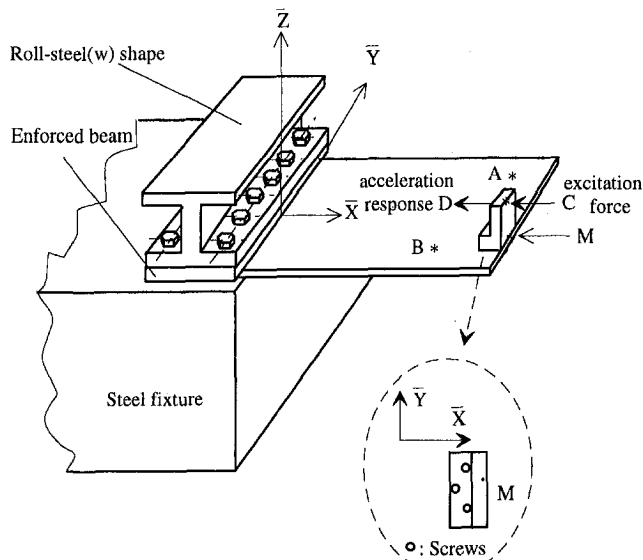


Fig. 1 Experimental set-up

response were measured simultaneously. The measured data were then transmitted through an IEEE interface to a PC computer. Using expressions (1) and (2), the rotational compliance of the plate was then computed.

3 Verification of the Experimental Set-up on a Single Plate

Before conducting the rotational compliance study, a single plate was first tested to compare the results with a finite element analysis. The hammer excitation was used to apply a driving force on the plate at point A (340, 110 mm) and the acceleration of the plate was measured at point B (300, -110 mm) (cf. Fig. 1). A finite element analysis was performed using I-DEAS, following the same method presented in the companion paper. The measured and computed response curves are compared in Fig. 3, in which the acceleration is expressed in decibel referenced to $1.0E-06 \text{ m/s}^2 \cdot \text{N}$ ($10 \log (T/1.0E-6)$). It can be observed that in the frequency range of interest, most of resonance peaks of the response curves coincide reasonably well. Furthermore, the amplitude difference is considered to be satisfactory for most frequencies. Phase angle data, though not presented for the sake of brevity, are also in agreement. Since relatively strong modal behavior is involved over such a wide frequency

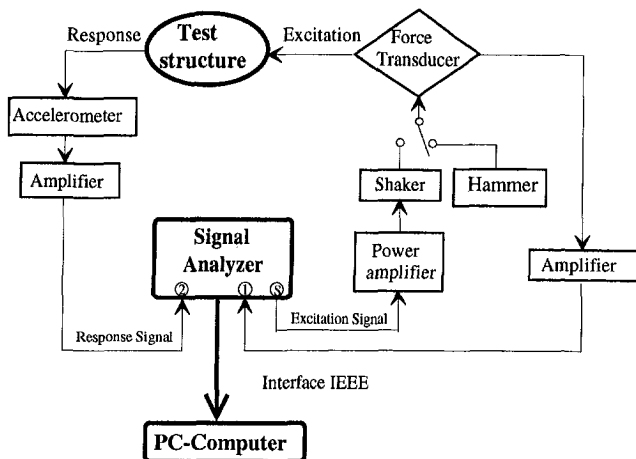


Fig. 2 Schematic block diagram of the measurements

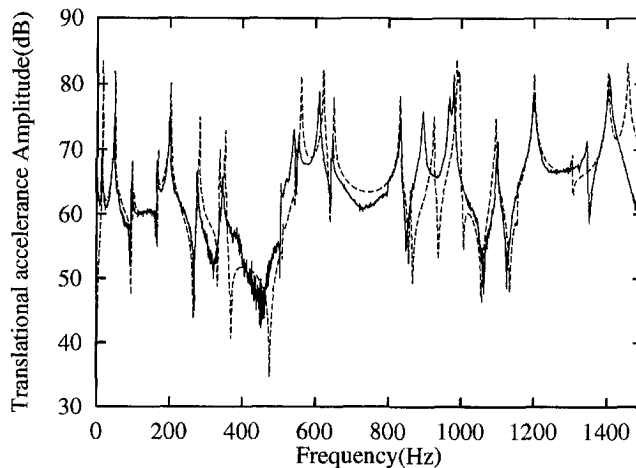


Fig. 3 Accelerance amplitude of a single plate: calculated value (—); measured value (---)

range, results are practically in agreement. These comparisons indicate that the tested plate is dynamically similar to the model and the clamped condition is properly performed.

4 Results and Discussions on Compliance Measurement

4.1 Force Correction. It is well known that when using either a shaker or an impact hammer, the real force applied to the structure differs more or less from the one measured by a force transducer, due to the exciting head separating the structure from the transducer. To obtain an accurate estimate of the real exciting force, some corrections are required. Figures 4a and 4b illustrate the excitation measurement set-up using, respectively, a hammer and an exciter. Both cases are represented by the equivalent dynamic model illustrated in Fig. 4c, where F_m and F_r are, respectively, the measured force and the real force

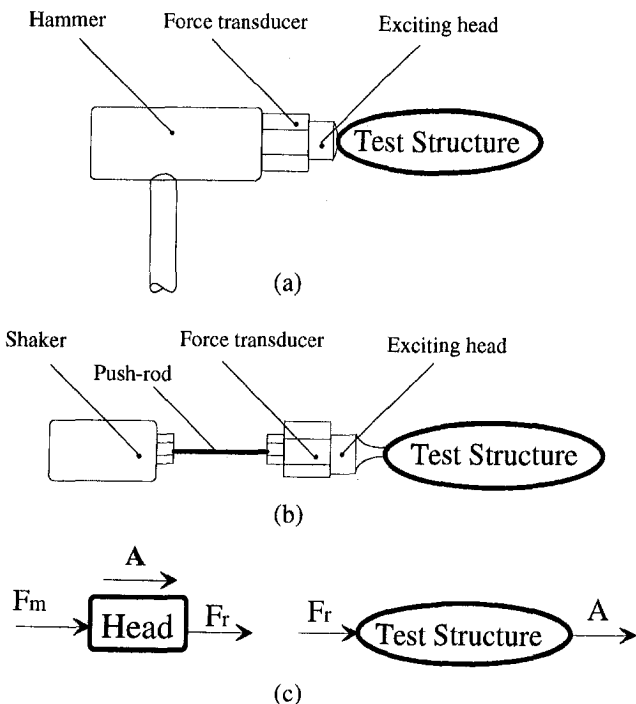


Fig. 4 Exciting force correction: (a) Hammer excitation; (b) Shaker excitation; (c) Dynamic model of excitations

applied to the structure. Let A be the measured acceleration and m_e , the total effective mass of the exciting head and the force transducer. The measured translational acceleration T_m is expressed as:

$$T_m = \frac{A}{F_m} \quad (3)$$

The real translational acceleration T_r should be:

$$T_r = \frac{A}{F_r} \quad (4)$$

Applying Newton's second law, the following simple relation exists:

$$F_m - F_r = m_e A \quad (5)$$

From Eqs. (3), (4) and (5) one obtains:

$$T_r = T_m / (1 - m_e T_m) \quad (6)$$

Eq. (6) provides a relationship between the measured and real translational acceleration for compliance correction purposes. In what follows, the above correction was applied. In all cases, the total mass of the exciting head and one half of the force transducer mass are added to obtain the effective mass m_e .

4.2 Mass Correction. Although a tiny accelerometer is used in the experiments, its mass should be considered for a precise evaluation of the compliance. Consequently, when calculating the tip moment of inertia I_{yy} , the accelerometer is considered as being part of the tip. The influence of the force transducer occurs only in the case of the shaker excitation because the force transducer is directly connected to the tip. In this case, the effective mass m_e is taken into account to precisely evaluate I_{yy} .

4.3 Excitation Methods. Any excitation method has advantages and limitations. Generally speaking, sinusoidal excitation with an exciter is used when high energy levels of excitation are required. Theoretically, the single-frequency slow-swept sine excitation is very accurate due to its controllable resolution, its high signal-to-noise ratio and its wide dynamic range. It is however time-consuming. In this regard, the broad band random and impact excitation methods are much more appealing. However, the low signal-to-noise ratio, aliasing and leakage problems decrease the measurement accuracy (Bendat and Piersol, 1985). The repeatability of the impact excitation is poor, whilst that of the broad band random excitation with an exciter is very good, so that in the former case a very large number of averages need to eliminate distortions and improve accuracy.

In this experiment, two types of excitations were investigated: broad band random and impact. In the case of random excitation, the exciting signal was limited to the frequency band from 1 Hz to 20 kHz by a band pass filter in the amplifier. In order to reduce the leakage errors and obtain a greater frequency resolution, Hanning windows and averages of several sequences were performed. The total response frequency range was set from 1 to 1600 Hz. Better results were obtained by dividing this frequency range into four subranges, 400 Hz wide. In the case of the impact excitation, the input force was directly applied with a hammer and an exponential window was used for the response measurements.

4.4 Translational Accelerance. The same basic configuration as the one defined in the companion paper was again used. As previously shown, measurement of the translational accelerance is needed to estimate the rotational compliance. Before the rotational compliance measurement was carried out, the translational accelerance was validated on the plate-tip combined structure.

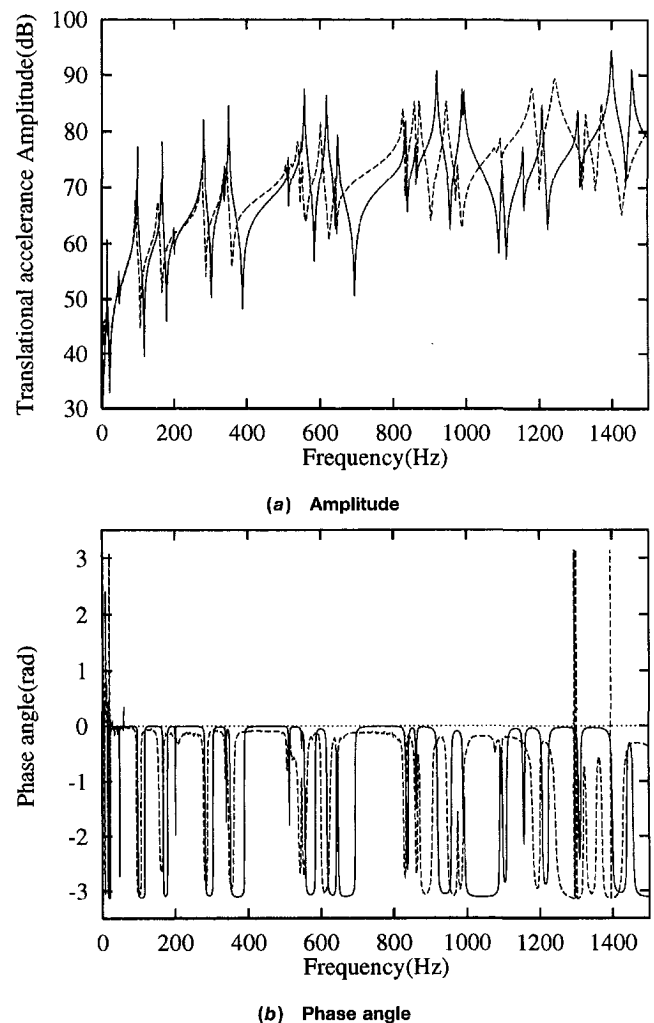
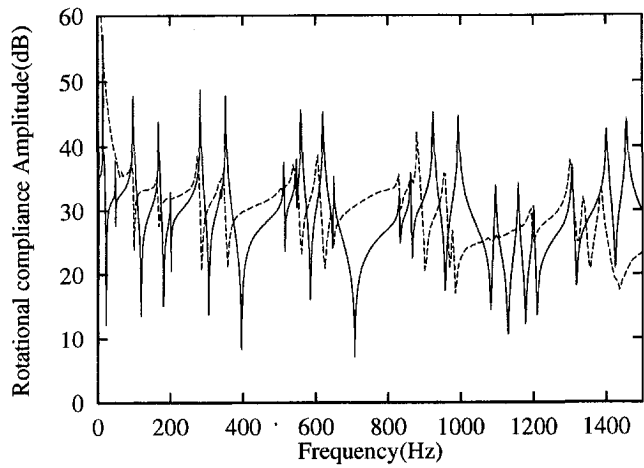


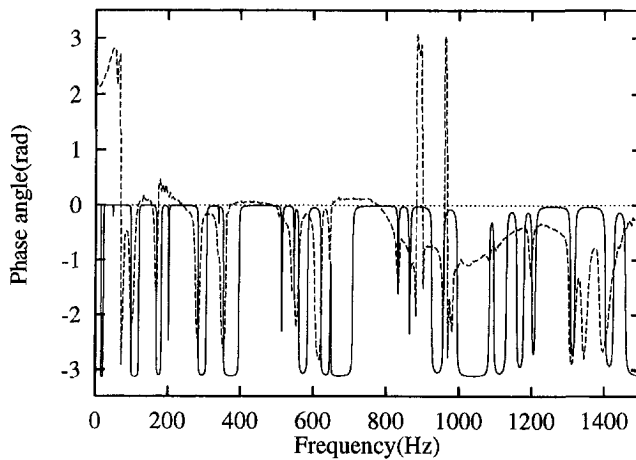
Fig. 5 Comparison of translational accelerance. Calculated value (—); measured value (---).

An exciter applied an exciting force at point C , and the response was evaluated at point D . Since the translational accelerance was under investigation, no tip correction was necessary. The measured translational accelerance amplitude and phase angle are compared with a finite element analysis in Fig. 5a and Fig. 5b respectively. The amplitude is expressed in dB referred to $1.0E-06 \text{ m/s}^2 \cdot \text{N}$ ($10 \log (A_{cr}/1.0E-6)$) and the phase angle in radians. It can be seen that there is good agreement in the case of both sets of results up to 900 Hz. Note that up to 15 modes occur in this range. Beyond this typical frequency (900 Hz), the positions of the resonance peaks diverge more significantly. Considerable effort has been made to improve this situation without any success. Since the calculations of rotational compliance is based on measurements of the translational accelerance, one must expect similar deviations for the rotational compliance data.

4.5 Rotational Compliance. Based on the translational accelerance data obtained above, the rotational compliance was determined. Again, the measured results were compared with finite element simulations. Two types of excitations were used. Figures 6a and 6b illustrate the results for impact excitation with a hammer, and Figs. 7a and 7b, for the random excitation with an exciter. From these graphs, one can clearly see that below 900 Hz, both the random and impact excitation curves are similar to the FEA curve: broadly speaking, most resonance peaks are well identified. The amplitude difference is reasonably small for most frequencies in the 0–900 Hz range. It should be



(a) Amplitude



(b) Phase angle

Fig. 6 Rotational compliance with hammer excitation. Expected value (—); measured value (---).

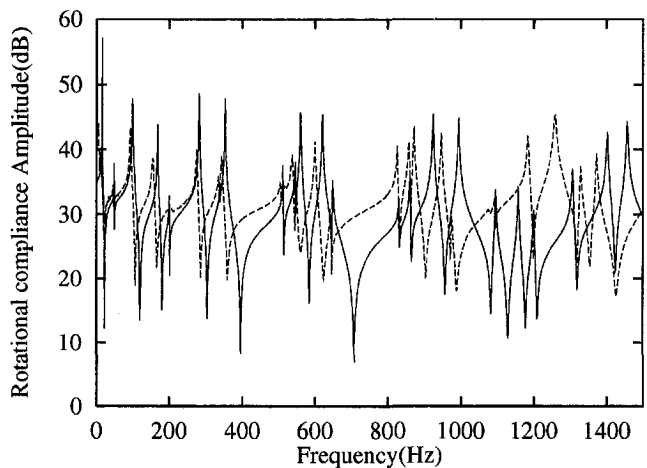
noted that the peak differences depend very much on the structural internal damping. As pointed out earlier, an identical damping ratio of 0.01 was used for all modes during numerical simulations. Actually, they may differ widely from one mode to another. Further comparison of the graphs shows variations in the results depending on the excitation methods. The random excitation seems to give better results than the impact one, at low to middle frequencies (below 900 Hz). In fact, in the case of hammer excitation, the input energy was insufficient at low frequencies so that the first two modes are missing. Moreover, resonance and anti-resonance response are not as clearly measured as in the case of random excitation. However, above 900 Hz, random excitation seems to have a greater influence on the system due to the attachment of the exciter. As a result, the compliance curves deviate more obviously from the expected value. A comparison between Figs. 6b and 7b shows that random excitation provides a more accurate phase angle measurement than an impact excitation. In conclusion, for the frequency range over which the technique can be considered to be valid (before 900 Hz in the present case), random excitations appears to be the appropriate choice.

The following example illustrates the effects of the tip attachment to the plate. During the development of the technique, we assumed that the tip was rigidly fixed to the plate and no damping existed at the interface. In the basic configuration used above, the tip was screwed to the plate using three small M3 bolts. Using random excitation, Fig. 8 compares the compliance

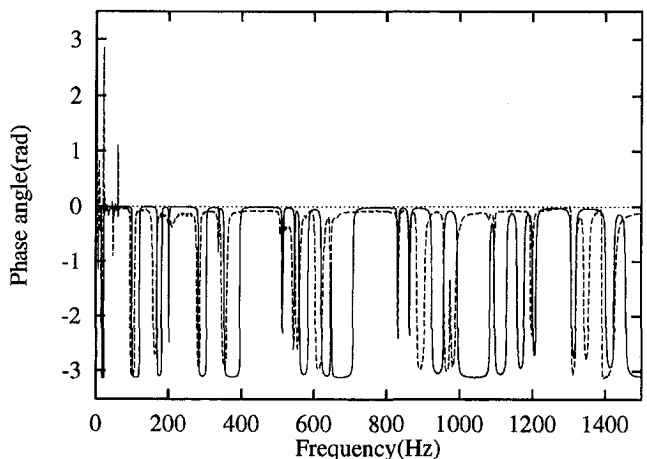
curves in terms of amplitude for the two following configurations: firstly the basic configuration already used previously; and secondly with the tip glued to the plate, using a high-strength metal glue before the three bolts were inserted. Addition of the glue enhances the rigidity of the tip-plate connection. Furthermore, if any relative motion should exist between the tip and the plate at the junction, the use of glue should bring additional damping to the system. It can be seen from Fig. 8 that, although small differences exist between the two curves, no appreciable improvement is obtained by using glue reinforcement. This observation suggests that three-point bolt connection provides sufficient rigidity. From a practical point of view, a glued connection without bolts would be much more convenient. However, based on preliminary tests, no suitable glue was found to ensure a rigid connection. This is certainly an interesting avenue to be explored further.

5 Compliance Sensitivity to Measured Quantities

In the estimation of the rotational compliance, the deviation of any one of the quantities in the compliance expressions will contribute to errors in rotational compliance. Errors introduced by the various assumptions and simplifications made during the analytical development have been analyzed using numerical simulations in the previous work. This section only focuses on errors associated with measured quantities. By following standard methods (Barry, 1978), an error analysis was performed on two measured quantities: the translational accelera-



(a) Amplitude



(b) Phase angle

Fig. 7 Rotational compliance with shaker excitation. Expected value (—); measured value (---).

tion and the excitation force. These can be described by three parameters: the amplitudes of the acceleration and the excitation force and the phase angle between them. By differentiating the compliance expressions (1) and (2) relative to the three parameters, the error expressions for the amplitude and phase angle can respectively be written as follows:

$$\frac{dA_{cr}}{A_{cr}} = \left(\frac{FA_a}{FA}\right) \frac{dA_0}{A_0} + \left(\frac{FA_f}{FA}\right) \frac{dF_0}{F_0} + \left(\frac{FA_\phi}{FA}\right) d\phi_a \quad (7)$$

$$d\phi_{cr} = \left(\frac{FF_a}{FF}\right) \frac{dA_0}{A_0} + \left(\frac{FF_f}{FF}\right) \frac{dF_0}{F_0} + \left(1 + \frac{FF_\phi}{FF}\right) d\phi_a \quad (8)$$

with

$$FA_a = -FA_f = \left(\frac{K}{T}\right)^2 - I_{yy} \frac{K}{T} \cos \phi_a$$

$$FF_a = -FF_f = -I_{yy} \frac{K}{T} \sin \phi_a \cos \phi_a$$

$$FA = \left(\frac{K}{T}\right)^2 - 2I_{yy} \frac{K}{T} \cos \phi_a + J_0^2$$

$$FF = \left(\frac{K}{T} \cos \phi_a\right)^2 - 2I_{yy} \frac{K}{T} \cos \phi_a + I_{yy}^2 (1 + \sin^2 \phi_a)$$

$$FA_\phi = -I_{yy} \frac{K}{T} \sin \phi_a$$

$$FF_\phi = I_{yy}^2 \cos \phi_a - I_{yy} \frac{K}{T} \quad (9)$$

Equations (7) and (8) can be expressed in the following abbreviated forms:

$$\epsilon(A_{cr}) = \frac{FA_a}{FA} \epsilon(A_0) + \frac{FA_f}{FA} \epsilon(F_0) + \frac{FA_\phi}{FA} \epsilon(\phi_a) \quad (10)$$

$$\epsilon(\phi_{cr}) = \frac{FF_a}{FF} \epsilon(A_0) + \frac{FF_f}{FF} \epsilon(F_0) + \left(1 + \frac{FF_\phi}{FF}\right) \epsilon(\phi_a) \quad (11)$$

where $\epsilon(A_{cr})$, $\epsilon(\phi_{cr})$ are respectively the errors of the amplitude and phase angle of the rotational compliance; $\epsilon(A_0)$ and $\epsilon(F_0)$ are respectively, the amplitude errors of the measured acceleration and force; and $\epsilon(\phi_a)$ is the error associated with the phase angle.

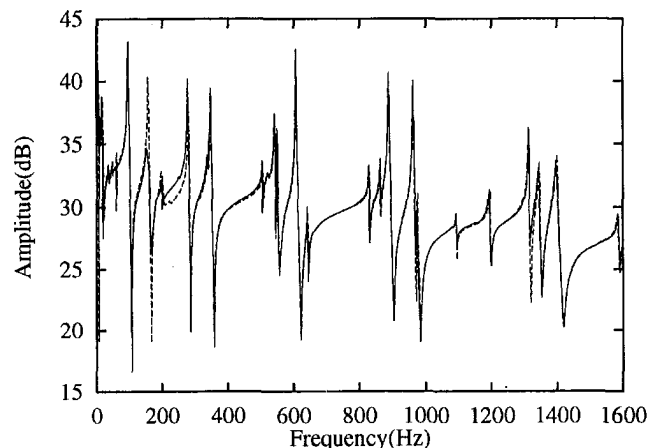
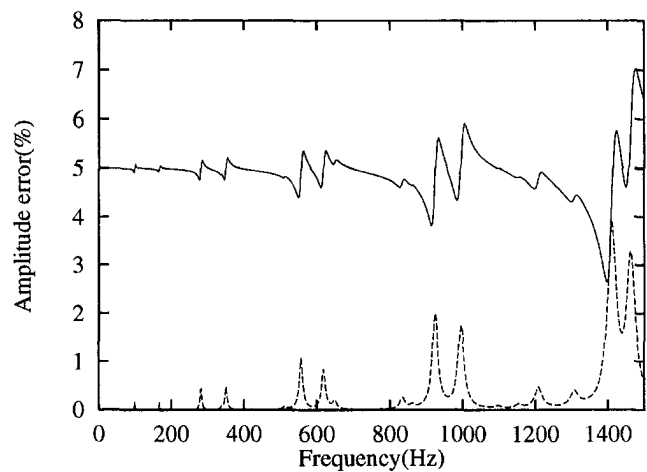
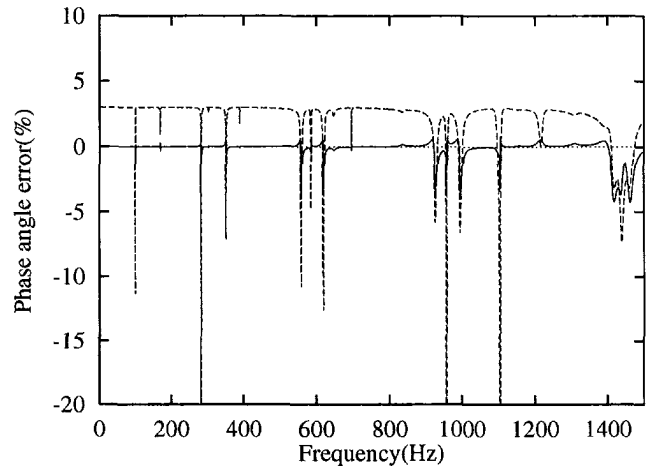


Fig. 8 Effects of connection on the amplitude of the rotational compliance. Without glue (—); with glue (---).



(a) Amplitude



(b) Phase angle

Fig. 9 Resulting errors on rotational compliance. Case 1: only 5% error on the acceleration amplitude (—); case 2: only 3° error on the acceleration phase angle (---).

On the basis of the above expressions, one can estimate the resulting error on the rotational compliance by introducing a slight deviation for each physical quantity. The first two expressions of Eq. (9) show that the amplitude error of the force affects the compliance estimation in the same way as the acceleration amplitude, and the opposite sign indicates a reverse effect. As a result, only the effects of the acceleration amplitude and phase angle error will be discussed. Two cases were considered: firstly, only the contribution of the amplitude error of the linear acceleration was considered by introducing $\epsilon(A_0) = 5.0$ percent without any phase error; secondly, a phase error of 3 deg ($\epsilon(\phi_a) = 3$ deg) was used without any amplitude variations. The resulting rotational compliance errors are represented in Fig. 9a for the amplitude, and in Fig. 9b, for the phase angle variations. Figure 9a shows that an acceleration amplitude error leads to a compliance amplitude error of the same order of magnitude, with visible fluctuations in the vicinity of the resonance peaks. On the other hand, a phase angle error does not fundamentally change the whole amplitude level of the compliance except around resonances. The effects of both amplitude and phase angle errors seem to be amplified at higher frequencies. The same analysis performed in terms of phase angle is illustrated in Fig. 9b. Broadly speaking, except in the vicinity of the resonances, the acceleration amplitude error does not strongly affect the phase angle. However, a phase angle error of the acceleration gives phase shifts of the same order of mag-

nitide. Once again, situations at resonance are controlled by both types of errors. It should be stressed that, due to the aforementioned similarity between the effects of the excitation force and those of acceleration, all conclusions reached regarding acceleration amplitude measurements apply equally to the force error effects.

6 Conclusions

The Tip Excitation Technique proposed in the companion paper (Cheng and Qu, 1997) was investigated experimentally. Using a typical structure, the experimental results show good agreement with finite element predictions below 900 Hz, including as many as 15 modes.

The following conclusions were obtained:

1) Different hypotheses made during the development of the technique are supported by real tests. The results demonstrate that the proposed technique is feasible for attached plane structures in the low to middle frequency range. Further improvements are still needed to increase measurement accuracy and to make the technique applicable to higher frequencies.

2) With the force and mass correction proposed in the present paper, both random and impact excitations can be used. Nevertheless, random excitation with an exciter seems to give better results.

3) A sufficiently rigid tip-plate attachment can be made using a three-point bolt connection.

4) In off-resonance zones, the accuracy of the compliance amplitude measurements depends mainly on the accuracy of both acceleration and force amplitude, whilst the phase angle of the compliance is mainly governed by the measurement of the acceleration-force phase angle. However, in the vicinity of resonances, all three types of errors (force amplitude, acceleration amplitude and phase angle) simultaneously affect the compliance measurement in terms of both amplitude and phase angle.

The present work is an attempt to tackle the rotational compliance measurement problem. As pointed out earlier, compliance

is usually used to predict the dynamic behavior of substructures in complex structure analyses. From this point of view, although further effort is still needed to improve the technique for better accuracy and wider frequency range, the technique can be applicable to various industrial applications. It provides an overall compliance estimation of structures exhibiting relatively strong modal behavior. Since the in-plane motion of the main structure is neglected in the analysis, the technique applies only to attached plane structures. The extension of the technique to the cross compliance measurements should not pose particular difficulties, except that an additional accelerometer should be used to measure the structure response at a point different from the excitation one.

Current work consists in extending the TET to curved structures with general boundary conditions. Since many common factors exist for both types of structures, the systematic assessment of the technique on the plane structure reported here should provide a solid foundation for further extension of the technique to more complex structures.

Acknowledgments

The authors wish to thank the National Science and Engineering Research Council of Canada and F.C.A.R. for supporting this work. We are grateful to the Ministry of Aeronautics and Astronautics of China and China Flight Test and Research Establishment for providing Y. C. Qu with financial support. We thank Professor John Dickinson for doing the revision in English of this paper.

References

- Cheng, L., and Qu, Y. C., 1997, "Rotational Compliance Measurement of a Flexible Plane Structure by Means of an Attached Beam-like Tip, Part 1: Method Development And Numerical Simulation," *ASME JOURNAL OF VIBRATION AND ACOUSTICS*, Vol. 119, pp. 596–602.
- Broch, J. T., 1984, *Mechanical Vibration and Shock Measurement*, 2nd Edition, B&K, Denmark.
- Bendat, J. S., and Piersol, A. G., 1985, *Random Data: Analysis and Measurement Procedures*, 2nd Edition, John Wiley & Sons, Inc., New York.
- Barry, B. A., 1978, *Errors in Practical Measurement in Science, Engineering, and Technology*, John Wiley & Sons, Inc., New York.